

BREAKING OF GRAVITY WAVES IN A NEIGHBORHOOD OF THEIR SECOND CRITICAL PROPAGATION SPEED

V. I. Bukreev, E. M. Romanov, and N. P. Turanov

UDC 532.59

Experimental data on gravity shallow-water waves generated by a vertical plate moving in a predetermined manner are given. The plate completely covers the cross section of the channel. It is found that with when the wave speed exceeds the first critical value known in hydraulics, the wave retains smoothness. Breaking of the waves begins at the second critical speed (which is about 1.3 times as high), whose value coincides with the limiting propagation speed of a solitary wave.

For a liquid layer at rest above an even horizontal bottom, there are, at least, two critical propagation speeds of gravity waves: $c_1 = \sqrt{gh}$ and $c_2 = \beta\sqrt{gh}$ (g is the acceleration of gravity, h is the depth of the layer, and $\beta > 1$). The second critical speed c_2 was detected by a theoretical analysis of solitary waves of limiting amplitude. Different mathematical models give different values of β . The second approximation of shallow-water theory yields $\beta = \sqrt{2}$ [1]. Using the complete equations of potential flow of a liquid, Longuet-Higgins and Fenton [2] obtained $\beta = 1.294$. The experiments of [3-5] showed that c_2 is critical not only for solitary waves and that the second of the indicated values of β is more accurate. In neighborhoods of c_1 and c_2 , the wave pattern changes greatly. In particular, the waves can break.

The present paper is a continuation of [5]. Here the emphasis is on the transition of smooth waves to breaking waves in a neighborhood of c_2 . Breaking of waves is a good object for experimental investigation of the fundamental problem of transition from order to partial or full chaos. In this case, it is much easier to combine tool measurements with visual observations than, for example, in studies of laminar-turbulent transition in a pipe or a boundary layer.

In the methodical respect, the experiments described here are similar to those in [5]. A rectangular channel with a horizontal bottom of length $L = 3.8$ m and width 20 cm was filled with water at room temperature. Waves were generated by translational displacement of one of the butt-end walls of the channel. The term "butt-end wall" is used here for the particular case of translational motion of the vertical plate which completely covers the cross section of the channel. This case is similar to the classical gas-dynamic problem of motion of a piston in a pipe with a compressible gas. The following law of motion of the wall is specified:

$$x_*(t) = \begin{cases} Ut + UT_1[\exp(-t/T_1) - 1] & \text{at } 0 \leq t < T_2, \\ l & \text{at } t \geq T_2, \end{cases} \quad y_*, z_* = \text{const.}$$

Here t is the time, x_* , y_* , and z_* are the coordinates of an arbitrary point of the moving wall, and U , T_1 , T_2 , and l are parameters. We used a fixed rectangular coordinate system x , y , z with origin on the line of intersection of the undisturbed free surface of the water and the moving wall at $t = 0$. The x axis is directed to the fixed butt-end wall of the channel, and the z axis is directed vertically upward. Only three of the four parameters of the law of motion are independent. In the experiments, $T_2 \gg T_1$, and we can assume with good accuracy that $l = U(T_2 - T_1)$.

Lavrent'ev Institute of Hydrodynamics, Siberian Division, Russian Academy of Sciences, Novosibirsk 630090. Translated from *Prikladnaya Mekhanika i Tekhnicheskaya Fizika*, Vol. 39, No. 2, pp. 52-58, March-April, 1998. Original article submitted July 8, 1996.

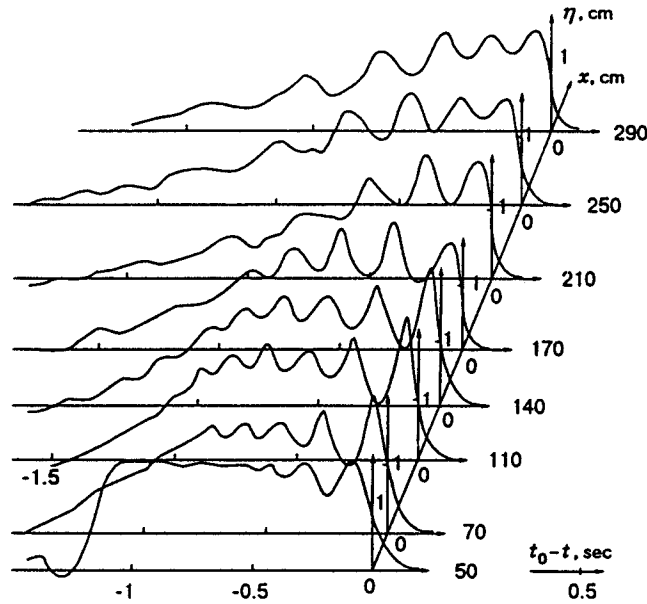


Fig. 1

The departure of the free surface of the water from the position of equilibrium η was measured by fixed wavemeters. Signals from the wavemeters were delivered to a specialized HISTOMAT-S computer and recorded by recorders. As long as the waves remained stable, they were plane, and, hence, the function η depended on x , t , and the four basic dimensionless parameters: L/h , U/\sqrt{gh} , $T_1\sqrt{g/h}$, and $T_2\sqrt{g/h}$. Below, information is given only for those t for which the reflected waves have not yet reached the point x considered and the influence of the parameter L/h has not been manifested. After loss of stability and breaking of the waves, fluctuations of η with respect to x , y , and t occurred, and the effect of physical quantities such as the density, viscosity, and compressibility of water and air and the surface-tension coefficient became pronounced.

We studied nonstationary waves. For nonstationary waves, it is necessary to define expressly the notion of the propagation speed c . In the experiments, c was determined as the speed of longitudinal motion of that point at the leading edge of the wave for which $\eta = \eta_m/2$, where η_m is the height of the first crest (Fig. 1). The value of c was calculated from the time Δt required for this point to travel the distance $\Delta x = 10$ cm between two fixed wavemeters. From results of repeated measurements under the same conditions, it was found that the relative standard deviation was not higher than 1.5% for η_m and 1% for c . The standard deviation of the derivative $\partial\eta/\partial t$ reached 10%.

Experiments were performed for several combinations of the parameters of the problem. Typical results are discussed in greater detail for an experiment with $h = 3.06$ cm, $U/\sqrt{gh} = 0.425$, $T_1\sqrt{g/h} = 2.15$, and $T_2\sqrt{g/h} = 33.7$ ($l/h = 13.4$). Figure 1 shows the dependence of η on $t_0 - t$ for several fixed values of x . Here t_0 is the time during which the point of the leading edge with $\eta = \eta_m/2$ reaches the point x considered ($h = 3.06$ cm, $U = 23.3$ cm/sec, $T_1 = 0.12$ sec, and $T_2 = 1.88$ sec). In this case, at $x = (110 \pm 5)$ cm, the first crest sharpened so that a portion of the liquid began to slide off the leading edge. At this instant, $c = c_2$ with good accuracy, and the height of the first crest has almost the largest value. Further, the rate of breaking increased rapidly, and at $x > 140$ cm, the head of the wave became similar to a classical hydraulic jump.

The evolution of the leading edge and first crest of the perturbation is illustrated in Fig. 2 in a coordinate system attached to the point $\eta = \eta_m/2$. The parameter values are the same as in Fig. 1; curves 1-5 correspond to $x/h = 16.3$, 35.9, 39.2, 45.8, and 56.7. Breaking began at $x/h = 35.9$ and became fully developed at $x/h = 45.8$. It is noteworthy that during development of the instability, the leading edge changed only slightly. The derivative $(1/c_2)\partial\eta/\partial t$ changed more markedly, as shown in Fig. 3 (the parameter values

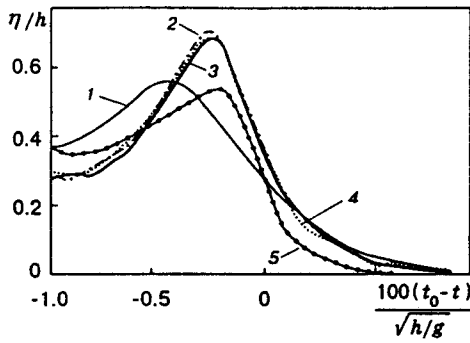


Fig. 2

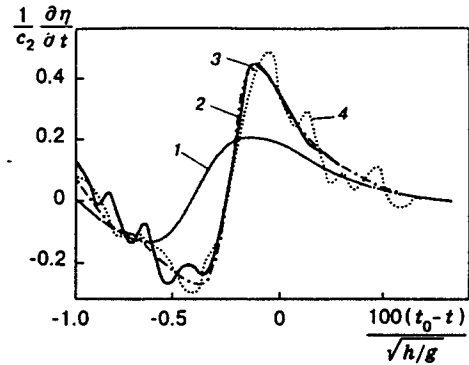


Fig. 3

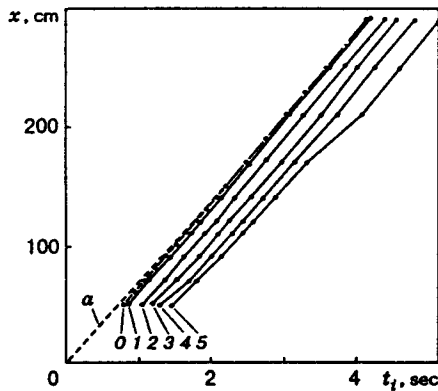


Fig. 4

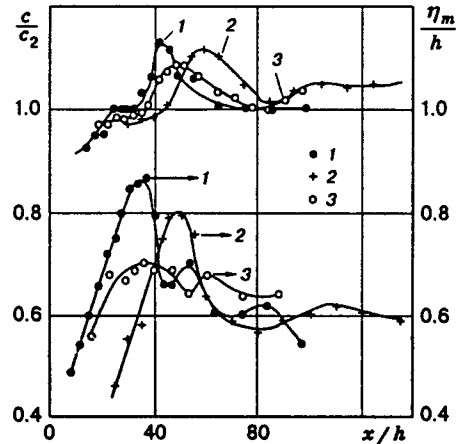


Fig. 5

are the same as in Fig. 2). A sensitive indication of the presence of instability is fluctuation of the derivative. Figure 3 shows that at $x/h = 35.9$, the plot of the derivative still remains smooth, and at $x/h = 39.2$, there are noticeable fluctuations in it.

At the beginning of breaking, the largest value of the dimensionless derivative was 0.43 ± 0.05 . In the dimensionless form adopted here, the derivative characterizes the slope of the free surface to the horizon. Measurements for other combinations of the parameters of the problem gave approximately the same value of the limiting slope of the leading edge (with the indicated measurement error).

Figure 4 gives information on the travel time $t_i(x)$ for a number of characteristic points on the wave profile. The number 0 is assigned to the point with $\eta = \eta_m/2$ (this is the previously determined t_0), and numbers 1-5 are assigned to wave crests beginning from the first crest at the leading edge. The slope of the straight line a to the axis t_i is equal to c_2 . The parameter values are the same as in Fig. 1. Analysis of $t_i(x)$ showed that the points 0 and 1 moved at a subcritical speed for $x/h < 35.9$ and at a supercritical speed for $x/h > 35.9$. In the interval $38 < x/h < 65$, the propagation speed of the second and third crests was 3-5% higher than c_2 , and outside of this interval it was lower than c_2 . The fourth and fifth crests moved at subcritical speeds all the time.

The effect of various parameters on the process of transition through c_2 is illustrated in Fig. 5, which shows the dependences of the height of the first crest η_m and the propagation speed c of the point with $\eta = \eta_m/2$ on x . Points 1-3 correspond to $h = 3, 3.06, \text{ and } 2 \text{ cm}$, $U/\sqrt{gh} = 0.509, 0.425, \text{ and } 0.422$, $T_1\sqrt{g/h} = 4.16, 2.15, \text{ and } 3.77$, and $T_2\sqrt{g/h} = 17.90, 33.66, \text{ and } 52.27$. In transition through the first critical speed c_1 , the waves remained stable and smooth in all three examples. Interestingly, with approach to c_2 from below, the

increase in the speed c was markedly decelerated and the height η_m continued to increase monotonically. The deceleration of increase in c is especially pronounced for curve 1. Figuratively speaking, the liquid accumulated ahead of the invisible barrier $c = c_2$ and then broke through it, and the speed c increased sharply again. Visual observations and data on the derivative $\partial\eta/\partial t$ showed that at precisely this moment the breaking process began. The largest value of η_m was attained somewhat later than the beginning of transition to the supercritical region of c . A similar result has been obtained [2] by a theoretical analysis of solitary waves of limiting amplitude.

For the method of wave generation adopted here, replenishment of the wave energy was performed only at $t < T_2$, whereas in breaking, a major portion of the mechanical energy of waves dissipated in heat. Therefore, in the supercritical region, the speed c reached a certain largest value and then decreased nonmonotonically. Fluctuations of the propagation speed of the leading edge of a breaking wave are known for a classical hydraulic jump.

In Fig. 5 (points 1), c approaches c_2 again from above, i.e., from the supercritical region. It is interesting that, despite the energy dissipation, the constant value $c = c_2$ was retained on a rather large interval x/h . On this interval, the reverse transition from a breaking wave to a smooth wave was observed.

The available insufficient information on the complex process of wave breaking in a neighborhood of c_2 can be generalized as follows.

In a sense, c_2 is more critical than c_1 . In particular, when $c > c_2$, the possibilities of such a stabilizing factor as the dispersion of small-amplitude harmonic waves are exhausted. In a neighborhood of c_1 , the loss of stability appears to follow a severe rigid type, i.e., the perturbation intensity should exceed a rather large threshold value. In a neighborhood of c_2 , the situation is different. It appears that here the loss of stability follows a mild pattern, i.e., theoretically infinitesimal perturbations are sufficient for the development of instability. In the region $c_1 < c < c_2$, there are smooth *stationary* waves such as cnoidal, solitary, or monoclinic waves. The existence of smooth *stationary* waves with $c > c_2$ is questionable.

Under certain conditions, the nonstationarity of waves can counteract the development of instability. The experiments performed have shown that for $c > c_2$, the effect of this factor is also weaker than for $c < c_2$. In experiments with $c < c_2$, it is easy to generate nonstationary waves that remain smooth up to complete degeneration because of molecular viscosity. In the region $c > c_2$, it is difficult to prevent breaking of nonstationary waves even in a physical experiment, where another strong stabilizing factor — surface tension — operates. We detected two cases where nonstationary waves with $c > c_2$ did not break. One of these cases is reported in [6]. With certain stipulations, the fact that the second and third crests of the wave in Fig. 1 propagated at $c > c_2$ and did not break can be regarded as the second example. In a private discussion, V. Yu. Lyapidevskii noted that the nonstationarity in this case manifests itself as a general change of the wave of a complex shape, so that its second and subsequent crests spread over the perturbed liquid. Visual observations showed that, although the second and third crests did not break, they were also unstable. The instability manifested itself in the existence of relatively small three-dimensional perturbations against the background of the main wave.

Surface tension is a fundamentally important stabilizing factor for both $c < c_2$ and $c > c_2$. It is known that when surface tension is ignored, the steady shear flow of two immiscible liquids of different density is absolutely unstable by the Kelvin–Helmholtz mechanism: no matter how small the difference in speed between the liquids, there are infinitesimal perturbations that grow with time, drawing energy from the main flow. The water–air system is not an exception, and only surface tension ensures stability of gravity waves on water even in the region $c < c_1$. In a neighborhood of c_2 , the effect of surface tension becomes even more pronounced. It hinders sharpening of wave crests and greatly affects the entrainment of air in water during wave breaking.

In a neighborhood of c_2 , at least three destabilizing factors operate. The first is the growth of infinitesimal perturbations. In our experiments, these perturbations originated on the butt-end walls of the channel and appeared as oblique waves against the background of the main wave. The growth of small perturbations was hindered by surface tension, and they did not lead to breaking. A second factor is sharpening of the wave crests similar to the sharpening that occurs in the limiting Stokes wave. In the experiments, at a certain stage of the process of sharpening, a portion of the liquid slid off the crest along the leading edge of the

TABLE 1

Values of the Function $\eta(t - t_*)$ for $h = 3.06$ cm, $U = 23.3$ cm/sec, $T_1 = 0.12$ sec, and $T_2 = 1.88$ sec

η , cm							
$x = 50$ cm, $t_* = 0.6$ sec							
0.040	0.05	0.08	0.12	0.19	0.28	0.40	0.58
0.81	1.07	1.36	1.60	1.67	1.57	1.38	1.21
1.12	1.11	1.20	1.34	1.53	1.60	1.56	1.50
1.43	1.39	1.44	1.51	1.60	1.57	1.50	1.52
1.58	1.60	1.59	1.59	1.58	1.57	1.55	1.57
1.60	1.61	1.62	1.61	1.59	1.58	1.58	1.59
1.60	1.61	1.61	1.62	1.62	1.63	1.64	1.64
1.65	1.65	1.65	1.64	1.51	1.54	1.41	1.24
1.02	0.76	0.52	0.27	0.10	0.00	-0.07	-0.07
-0.04	-0.03	0.04	0.16	0.25	0.22	0.19	0.10
$x = 110$ cm, $t_* = 1.4$ sec							
0.00	0.00	0.01	0.02	0.02	0.02	0.03	0.04
0.06	0.10	0.18	0.31	0.51	0.81	1.26	1.87
2.10	1.79	1.43	1.15	0.98	0.85	0.85	1.10
1.21	1.59	1.80	1.79	1.65	1.36	1.29	1.20
1.27	1.36	1.43	1.61	1.65	1.55	1.49	1.43
1.34	1.36	1.43	1.53	1.71	1.74	1.55	1.43
1.41	1.41	1.48	1.59	1.63	1.55	1.44	1.34
1.30	1.37	1.42	1.33	1.22	1.10	1.03	1.02
1.02	0.93	0.82	0.73	0.68	0.64	0.63	0.61
0.55	0.49	0.45	0.40	0.36	0.32	0.27	0.25
0.22	0.19	0.16	0.13	0.22	0.19	0.16	0.13
0.10	0.08	0.05	0.02	-0.01	-0.03		
$x = 250$ cm, $t_* = 3.4$ sec							
0.02	0.03	0.03	0.04	0.10	0.20	0.36	0.67
1.30	1.54	1.60	1.55	1.43	1.32	1.26	1.29
1.35	1.44	1.55	1.61	1.57	1.44	1.29	1.16
1.09	1.10	1.21	1.42	1.61	1.70	1.67	1.53
1.33	1.15	1.04	0.98	1.00	1.08	1.17	1.25
1.31	1.40	1.42	1.33	1.18	1.04	0.93	0.85
0.82	0.84	0.85	0.83	0.82	0.85	0.90	0.96
1.01	1.00	0.93	0.83	0.76	0.72	0.69	0.65
0.59	0.53	0.50	0.52	0.55	0.58	0.59	0.58
0.57	0.57	0.57	0.58	0.58	0.56	0.53	0.48
0.43	0.38	0.32	0.29	0.28	0.28	0.31	0.34
0.34	0.33	0.30	0.26	0.23	0.21	0.22	0.24
0.26	0.27	0.26	0.24	0.20	0.17	0.14	0.13
0.14	0.14	0.14	0.11	0.05	0.01	0.00	0.01

Note. The argument t increases from left to right in the rows with a step $\Delta t = 0.02$ beginning from t_* .

wave like an avalanche. A third destabilizing factor is the nonlinear effect due to the fact that the propagation speed of the leading edge of the traveling wave increases from the trough to the crest. With attainment of a certain limiting slope, for which a measure can be the above-mentioned derivative, overturning of the leading edge with intense mixing of water and air occurred in the experiments.

The indicated mechanisms for the loss of stability have been analyzed theoretically for waves of specific types, for example, steady waves. Theory gives well-defined relations between wave characteristics such as the length, amplitude, slope, etc. In this case, it makes no sense to discuss which characteristic should be preferred in the detection of critical situations. The notion of a critical wave number is most frequently used for linear harmonic waves, the notion of a limiting amplitude is used for solitary waves, and the notion of a limiting slope for highly nonlinear waves. However, for waves of a more general type, including the waves considered in the present paper, the choice of an appropriate characteristic is significant. Of course, in this case too, there is a relationship between various characteristics, but it is not universal and, as a rule, is not known beforehand. For example, in the experiments, the limiting height of the first wave crest depended on the combination of the initial parameters and was either larger or smaller than the limiting amplitude of a solitary wave, (Fig. 5). At the same time, the propagation speed at which breaking began was the same and equal to c_2 , the maximum propagation speed of a solitary wave. This versatility has a fundamental physical basis and can be used as a postulate for various purposes.

In most of the modern analytical and numerical methods used to investigate gravity waves, smooth and discontinuous solutions of equations are studied independently of each other. Calculations for smooth waves are performed up to the moment of loss of stability, and in calculations of discontinuous waves, the initial data are specified ignoring their previous evolution in a smooth form. Lyapidevskii [7] proposed a mathematical model that permits describing the development of a perturbation from a state of rest to breaking waves. The problem of the motion of the butt-end wall of a channel is a good object for testing such models. Therefore, we give a table of experimental data for the function $\eta(t - t_*)$, where t_* is such that $\eta = 0$ for $t < t_*$.

This work was supported by the Russian Foundation for Fundamental Research (Grant No. 95-01-01164).

REFERENCES

1. L. V. Ovsyannikov, N. I. Makarenko, and V. I. Nalimov, *Nonlinear Problems of the Theory of Surface and Internal Waves* [in Russian], Nauka, Novosibirsk (1985).
2. M. S. Longuet-Higgins and J. D. Fenton, "On the mass, momentum, energy, and circulation of a solitary wave. II," *Proc. Roy. Soc., London*, **A340**, 471-493 (1974).
3. E. S. Chan and W. K. Melville, "Deep-water plunging breakers: a comparison between potential theory and experiments," *J. Fluid Mech.*, **189**, 423-442 (1988).
4. J. Sander and K. Hutter, "Evolution of weakly nonlinear shallow water waves generated by a moving boundary," *ACTA Mech.*, **91**, 119-155 (1992).
5. V. I. Bukreev and N. P. Turanov, "Experiments with shallow-water waves generated by the motion of the butt-end of a channel," *Prikl. Mekh. Tekh. Fiz.*, **37**, No. 6, 44-50 (1996).
6. V. I. Bukreev and A. V. Gusev, "Waves generated by a body falling on the free surface of shallow water. Experiment," *Dokl. Ross. Akad. Nauk*, **341**, No. 6, 761-763 (1995).
7. V. Yu. Lyapidevskii, "Equations of shallow water with dispersion. A hyperbolic model," *Prikl. Mekh. Tekh. Fiz.*, **39**, No. 2, 40-46 (1998).